Evolution of the Dislocation Structure During Compression in a Mg–Zn–Y Alloy with Long Period Stacking Ordered Structure

Kristian Máthis, Moustafa El-Tahawy, Gerardo Garcés, and Jenő Gubicza

Abstract

Evolution of the dislocation structure in $Mg_{97}Y_7Zn_5$ (at. %) alloy having long period stacking ordered (LPSO) structure was studied during compression tests. Two materials, an as-cast and an extruded one were deformed up to the applied strain of ~25%. The evolution of the crystallite size, the dislocation density and the population of the particular slip systems were determined by the evaluation of the X-ray diffraction peak profiles. A very low dislocation density with the order of magnitude 10^{12}–10^{13} m^{-2} was detected in the compressed specimens. This dislocation density did not increase considerably with increasing strain. At the same time, a significant decrease of the crystallite size occurred during compression. These observations can be explained by the arrangement of dislocations into low energy dipolar configurations, such as kink walls, which do not contribute to the dislocation density measurable by X-ray diffraction peak profile analysis, however they yield a fragmentation of the crystallites.

Keywords

LPSO structure • Diffraction line profile analysis
Dislocation density • Non-basal slip

K. Máthis (✉)
Department of Physics of Materials, Faculty of Mathematics and Physics, Charles University, Ke Karlovu 5, 121 16 Prague, Czech Republic
e-mail: mathis@met.mff.cuni.cz

M. El-Tahawy · J. Gubicza
Department of Materials Physics, Faculty of Science, Eötvös Loránd University, Pázmány P. Sétány 1/A, 1117 Budapest, Hungary

M. El-Tahawy
Department of Physics, Faculty of Science, Tanta University, 31527 Tanta, Egypt

G. Garcés
Department of Physical Metallurgy, CENIM-CSIC, Avenida Gregorio Del Amo 8, 28040 Madrid, Spain

Introduction

Magnesium alloys with long-period stacking ordered (LPSO) structure belong to the new class of lightweight alloys, offering excellent strength-to-weight ratio. The high mechanical performance is ensured by the LPSO phase, which acts as short-fiber reinforcement, similarly to the composite materials [1]. The final strength is influenced particularly by the manufacturing parameters (e.g., extrusion ratio, rate and temperature) and the volume content and crystallographic structure of the LPSO phase. Many polytypes of LPSO phase was reported, including 10H, 14H, 18R and 24R [2], where the H and R refer to the hexagonal or rhombohedral symmetry, respectively, and the numbers indicate the periodicity of the structure. In general, the LPSO structures consist of combination of hexagonal closed packed Mg and Y or Zn enriched layers. The latter have a local face-centered cubic stacking sequence on the close packed planes [3]. There is a general agreement that one of the main deformation mechanisms in the LSPO phase is the so-called kinking, when wedge-like bands forms in the structure as a consequence of correlated movement of basal <*a*>-type dislocation dipoles. However, molecular dynamics simulations of Matsumoto et al. indicates that several further mechanisms should be considered, including twinning and non-basal slip [4]. The available experimental observations are usually performed by scanning-(SEM) or transmission electron microscopy (TEM) [5]. The results partially confirm the theoretical calculations, but the investigation at higher strain levels is rather difficult owing to the high dislocation density. The X-ray diffraction line profile analysis (XLPA) has been found as a reliable method for the investigation of the dislocation structure [6]. During the data processing, the experimental profiles are evaluated for the dislocation density, crystallite size or dislocation population in the particular slip systems [7, 8]. A doubtless advantage of this approach is the significantly larger investigated sample volume than that for TEM. In addition, XLPA is a

D. Orlov et al. (eds.), *Magnesium Technology 2018*, The Minerals, Metals & Materials Series, https://doi.org/10.1007/978-3-319-72332-7_60

non-destructive testing method. Thus, the sample preparation does not alter the dislocation structure formed during deformation.

In the present work, we studied the evolution of the dislocation structure in $Mg_{97}Y_7Zn_5$ (at. %) alloy, where the volume content of LPSO phase is very high (about 85%). Compression tests on both the as-cast and extruded samples were performed. The influence of the initial microstructure on the dislocation structure is discussed in detail.

Experimental

The $Mg_{97}Y_7Zn_5$ (at.%) alloy used for this study was prepared by melting of high purity elements Mg, Y and Zn and a Mg-22%Y (wt%) master alloy in a graphite crucible coated with boron nitride under a protective Ar atmosphere. A part of the ingot was further extruded at 350 °C with an extrusion ratio of 18:1. Rectangular samples with the cross section of 5 mm × 5 mm and a height of 8 mm were cut parallel and perpendicular to the longitudinal axis of the casted and extruded specimens for compression tests. The compression experiments were performed at room temperature and an initial strain rate of 10^{-3} s^{-1} for the engineering strains of ~5 and ~25% using an MTS 810 universal mechanical testing machine. The list of the samples is shown in Table 1. It is noted that for the extruded samples the samples failed before the desired maximum strain of 25% was achieved. Therefore, for the extruded samples compressed parallel and perpendicular to the extrusion direction the maximum strains were ~21 and ~13, respectively. The dislocation structures in the LPSO phase for the compressed specimens were studied by XLPA. The surface of the samples was mechanically polished and etched before the X-ray experiments. The diffraction peaks were measured on the surfaces lying parallel to the compression direction by a high-resolution rotating anode diffractometer (type: RA-MultiMax9, manufacturer: Rigaku) using CuKα_1 radiation with a wavelength of $\lambda = 0.15406$ nm. The line profiles were evaluated for the crystallite size, the dislocation density and the fractions of different slip systems using the modified Williamson-Hall method.

Results

Figure 1 shows a part of the X-ray diffraction pattern obtained on sample Extr-PA-5%. Both Mg and LPSO phases were detected. The structure of the major LPSO phase was identified as 18R. The fractions of the LPSO and Mg phases were 85 and 15% respectively. The lattice constants obtained from the peak positions are listed in Table 2. The peaks of the LPSO phase are broad which may be caused either by the small crystallite size or the significant density of dislocations formed during extrusion and compression. These two effects can be separated by the modified Williamson-Hall method. In this procedure, the integral breadth or the Full Width at Half Maximum (FWHM) of the peaks are plotted as a function of the product of square of the magnitude of the diffraction vector (g) and the dislocation contrast factor ($\overline{C}_{hkl}$) in accordance with the following equation [9].

$$FWHM = \frac{0.9}{d} + \Omega^* g^2 \overline{C}_{hkl} + O\left(g^4 \overline{C}_{hkl}^2\right), \qquad (1)$$

where d is the volume-weighted mean column length in the crystallites (it can be regarded as an apparent crystallite size), Ω^* depends on both the density and arrangement of dislocations and O stands for higher order terms in $g^2\overline{C}_{hkl}$. The magnitude of the diffraction vector can be obtained as $g = 2\sin\theta/\lambda$ where θ is the half of the Bragg angle of the diffraction peak. The dislocation contrast factor, $\overline{C}_{hkl}$, can be expressed as:

$$\overline{C}_{hkl} = \overline{C}_{hk0}\left(1 + q_1 z + q_2 z^2\right), \qquad (2)$$

where q_1 and q_2 are two parameters depending on the anisotropic elastic constants of the crystal and the type of dislocation slip system. $z = (2/3)(l/ga)^2$, where a is the

Table 1 The samples and their notations studied in this work

Sample name	Description
As-cast-PA-5%	As cast material, compressed parallel to the cast direction for the strain of 5%
As-cast-PA-25%	As cast material, compressed parallel to the cast direction for the strain of 25%
As-cast-PE-5%	As cast material, compressed perpendicular to the cast direction for the strain of 5%
As-cast-PE-25%	As cast material, compressed perpendicular to the cast direction for the strain of 25%
Extr-PA-5%	Extruded material, compressed parallel to the extrusion direction for the strain of 5%
Extr-PA-21%	Extruded material, compressed parallel to the extrusion direction for the strain of 21%
Extr-PE-5%	Extruded material, compressed perpendicular to the extrusion direction for the strain of 5%
Extr-PE-13%	Extruded material, compressed perpendicular to the extrusion direction for the strain of 13%

PA—parallel, *PE*—perpendicular direction with respect to the cast and extrusion axes

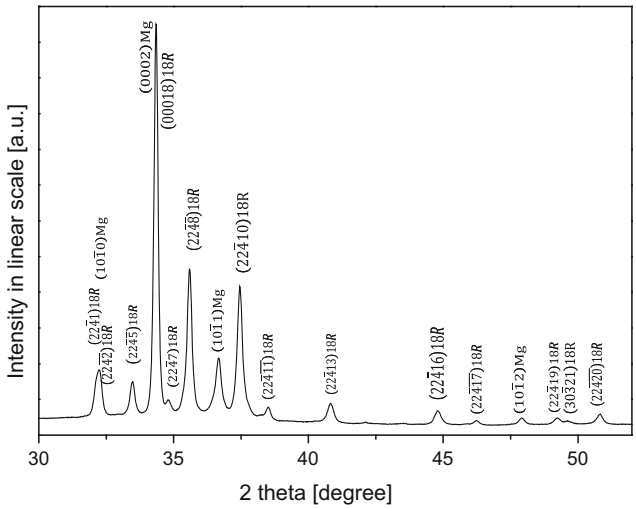

Fig. 1 A part of the X-ray diffractogram obtained on sample Extr-PA-5%. The indices of reflections for the LPSO and Mg phases are given above the peaks

lattice constant in the basal plane. $\overline{C}_{hk0}$ is the average dislocation contrast factor of the *hk0* type reflections. The values of $\overline{C}_{hk0}$, q_1 and q_2 are listed for the eleven most common slip systems of the 18R LPSO phase in Table 3. We note that this is the first study reporting these contrast factor values which were calculated by the ANIZC software [6] using the single crystalline elastic constants listed in Table 2.

Figure 2 shows the modified Williamson-Hall plot for sample Extr-PA-5%. Only those LPSO peaks were used in this evaluation procedure which do not overlap strongly with Mg peaks or other LPSO reflections. It is noted that the FWHM values were corrected for the instrumental broadening. The instrumental correction of the peak breadth was performed in accordance with the method described in [9] using the profile widths measured on LaB_6 standard material. The values of q_1 and q_2 in Eq. (2) are fitted in the modified Williamson-Hall plot in order to get the most smooth arrangement of the datum points along a straight line. From the comparison of the experimental values of q_1 and q_2 with the theoretical values listed for the different slip systems in Table 3, the fractions of <a>, <c> and <c + a> -type dislocations were determined using the method described in details in [8]. It was found that for all compressed samples studied in this work the majority of dislocations is of <a>-type with the fractions between 70 and 96%. The rest of dislocations is of <c + a> -type with the fraction of 4–30%. The amount of <c> dislocations is negligible. The intercept and the slope of the straight line fitted to the data points in the modified Williamson-Hall plot can be used for the estimation of the apparent crystallite size and the dislocation density, respectively [see Eq. (1)]. The slope of the straight line in the modified Williamson-Hall plot, Ω^*, is proportional to $\rho \times b^2$, where ρ is the dislocation density and b is the Burgers vector [9]. For all the samples studied in this work, the slope was 0.0003 ± 0.0001 nm, except for the as-cast specimens compressed for the strain of 5%, as for the latter samples the crystallite size and the dislocation density were larger and smaller, respectively, than the detection limits of the present X-ray line profile analysis. Therefore, the modified Williamson-Hall could not be applied for these samples. The slope of the modified Williamson-Hall plots determined for the other LPSO samples (0.0003 ± 0.0001 nm) was similar to that obtained for other Mg alloys with the dislocation density of $\sim 10^{14}$ m^{-2} [11]. However, for the LPSO phase the Burgers vector is larger with a factor of 3–7 than for the common Mg alloys (such as for AX41 or AZ31), due to the much larger lattice constants of the LPSO material. It is noted that the average Burgers vectors for the different specimens were calculated from the fractions of <a>, <c> and <c + a> -type dislocations and their values were found to be 1–2 nm. Since the slope of the straight line in the modified Williamson-Hall plot is proportional to ρ b^2, a similar slope in the modified Williamson-Hall plot for the LPSO phase corresponds to a one-two orders of magnitude lower dislocation density than that in the mentioned Mg alloys. Therefore, the estimated dislocation density in the present LPSO specimens is 10^{12}–10^{13} m^{-2}. It is noted that the order of magnitude of the dislocation density was the same in the extruded samples for both low and high strains as well as for the as-cast specimens compressed up to the strain of $\sim 25\%$.

Although, in the extruded samples the dislocation density measurable by X-ray line profile analysis did not change considerably with increasing strain, there was a decrease in the crystallize size (see Table 4) which indicates dislocation activity during compression. The dislocation structures with strongly shielded strain fields, such as small dipoles, cannot be detected by X-ray line profile analysis. Former studies [12] suggested the formation of kink walls during deformation of hexagonal materials. If the spacing between the dislocations with opposite signs in the kink walls is small, the strain field of these dislocations are strongly shielded, therefore they are practically invisible by X-ray line profile analysis. However, these kink walls result in a fragmentation

Table 2 The lattice constants (a and c) of the LPSO phase and its elastic constants taken from Ref. [10]

a (nm)	c (nm)	C_{11} (GPa)	C_{12} (GPa)	C_{13} (GPa)	C_{33} (GPa)	C_{44} (GPa)
1.118	4.694	68.4	25.8	19.6	75.2	21.6

Table 3 The dislocation contrast factors calculated for the eleven dislocation slip system in the LPSO phase

Notation	Burgers vector type	Burgers vector	Slip plane	$\bar{C}_{hk0}$	q_1	q_2
PrE	<a>	$1/3\langle\bar{1}2\bar{1}0\rangle$	$\{\bar{1}0\bar{1}0\}$	0.334	−0.1702	0.0072
PrE	<a>	$1/3\langle\bar{1}2\bar{1}0\rangle$	$\{10\bar{1}1\}$	0.327	−0.1630	0.0066
BE	<a>	$1/3\langle\bar{1}2\bar{1}0\rangle$	{0001}	0.2016	−0.0016	−0.0041
S1	<a>	$1/3\langle\bar{1}2\bar{1}0\rangle$	n.a.	0.1259	0.1654	−0.0213
Pr2E	<c>	$\langle 0001\rangle$	$\{1\bar{1}00\}$	0.03622	0.8318	0.0245
S3	<c>	$\langle 0001\rangle$	n.a.	4×10^{-6}	−4450	29552
Pr3E	<c + a>	$1/3\langle\bar{2}113\rangle$	$\{01\bar{1}0\}$	0.04081	0.0259	1.3281
Py3E	<c + a>	$1/3\langle\bar{2}113\rangle$	$\{1\bar{2}11\}$	0.04533	0.0320	1.0262
Py4E	<c + a>	$1/3\langle\bar{2}113\rangle$	$\{10\bar{1}0\}$	0.0485	0.6871	−0.0072
Py2E	<c + a>	$1/3\langle\bar{2}113\rangle$	$\{2\bar{1}\bar{1}2\}$	0.0451	0.6326	0.0175
S2	<c + a>	$1/3\langle\bar{2}113\rangle$	n.a.	0.0249	2.6611	−0.2191

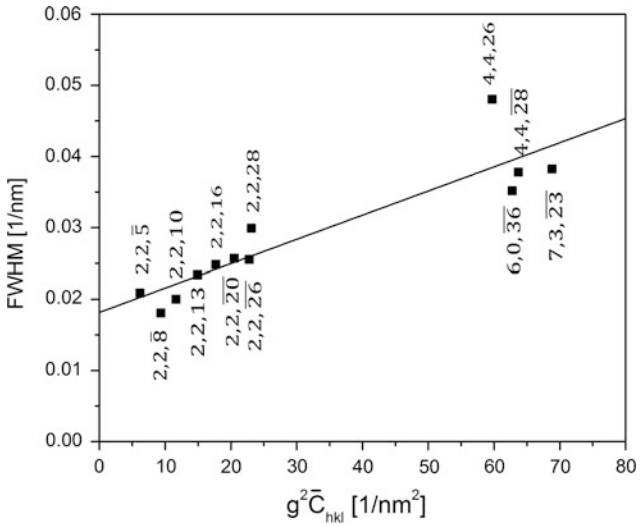

Fig. 2 The modified Williamson-Hall plot for sample Extr-PA-5%

of grains into smaller coherently scattering domains, i.e., the dislocations in the kink walls can be observed indirectly by the reduction of the crystallite size measurable by X-ray peak profile analysis. Therefore, according to our experiments it seems that there was a dislocation multiplication during compression of the LPSO samples, however a part of dislocations were arranged into low energy kink walls. This process yielded an unchanged low value of the dislocation density (10^{12}–10^{13} m^{-2}) obtained by X-ray peak profile analysis and a reduction of the apparent crystallite size. The low value of the dislocation density in the compressed LPSO samples can be attributed to the large Burgers vector, which yields a high shear strain during gliding even if the dislocation density is small. It should also be noted that this is the first study in the literature, which reports the type and density of dislocations in plastically deformed LPSO phase.

Summary

In this work, the evolution of the dislocation structure in as-cast and extruded magnesium alloys with 85% LPSO volume content was studied. The following conclusions can be drawn:

- The dislocation density was in the order of 10^{12}–10^{13} m^{-2} after the compression of the extruded samples up to the strain of ~5%. The dislocation density did not change considerably with increasing the strain to ~25%. Similar dislocation density value was observed for the

Table 4 The crystallite size of the LPSO phase for the different samples

Sample name	Crystallite size (nm)
As-cast-PA-5%	n.a.
As-cast-PA-25%	42 ± 4
As-cast-PE-5%	n.a.
As-cast-PE-25%	39 ± 4
Extr-PA-5%	56 ± 6
Extr-PA-21%	37 ± 4
Extr-PE-5%	49 ± 5
Extr-PE-13%	33 ± 3

as-cast LPSO materials compressed to the strain of ~25%, i.e., the dislocation density was not sensitive to the initial state of material.

- Although, the dislocation density measurable by X-ray line profile analysis did not change considerably with increasing strain, the crystallite size decreased which can be explained by the arrangement of dislocations into kink walls. The majority of dislocations was found to be of <a>-type with the fractions between 70 and 96% for the different samples. The rest of dislocations is of <c + a> -type with the fractions of 4–30%.

Acknowledgements The authors are grateful for the support of the Czech Grant Agency under grant Nr. 16-12075S.This work was supported by the Hungarian Scientific Research Fund, OTKA, Grant no. K-109021.

References

1. Matsuda, M, Ii, S, Kawamura, Y, Ikuhara, Y and Nishida, M, (2005) Variation of long-period stacking order structures in rapidly solidified Mg97Zn1Y2 alloy. Mater. Sci. Eng. A 393: 269–274.
2. Nie, JF, Zhu, YM and Morton, AJ, (2014) On the Structure, Transformation and Deformation of Long-Period Stacking Ordered Phases in Mg-Y-Zn Alloys. Metallurgical and Materials Transactions A 45a: 3338–3348.
3. Zhu, YM, Weyland, M, Morton, AJ, Oh-Ishi, K, Hono, K and Nie, JF, (2009) The building block of long-period structures in Mg–RE–Zn alloys. Scripta Mater. 60: 980–983.
4. Matsumoto, R and Uranagase, M, (2015) Deformation Analysis of the Long-Period Stacking-Ordered Phase by Using Molecular Dynamics Simulations: Kink Deformation under Compression and Kink Boundary Migration under Tensile Strain. Mater. Trans. 56: 957–962.
5. Yamasaki, M, Hagihara, K, Inoue, S, Hadorn, JP and Kawamura, Y, (2013) Crystallographic classification of kink bands in an extruded Mg–Zn–Y alloy using intragranular misorientation axis analysis. Acta Mater. 61: 2065–2076.
6. Borbély, A, Dragomir-Cernatescu, J, Ribárik, G and Ungár, T, (2003) Computer program ANIZC for the calculation of diffraction contrast factors of dislocations in elastically anisotropic cubic, hexagonal and trigonal crystals. J. Appl. Cryst. 36: 160–162.
7. Máthis, K, Gubicza, J and Nam, N, (2005) Microstructure and mechanical behavior of AZ91 Mg alloy processed by equal channel angular pressing. J. Alloy Comp. 394: 194–199.
8. Máthis, K, Nyilas, K, Axt, A, Dragomir-Cernatescu, I, Ungár, T and Lukáč, P, (2004) The evolution of non-basal dislocations as a function of deformation temperature in pure magnesium determined by X-ray diffraction. Acta Mater. 52: 2889–2894.
9. Gubicza, J, (2014) X-ray line profile analysis in materials science. IGI Global, Hershey.
10. Tane, M, Kimizuka, H, Hagihara, K, Suzuki, S, Mayama, T, Sekino, T and Nagai, Y, (2015) Effects of stacking sequence and short-range ordering of solute atoms on elastic properties of Mg–Zn–Y alloys with long-period stacking ordered structures. Acta Mater. 96: 170–188.
11. Krajňák, T, Minárik, P, Stráská, J, Gubicza, J, Máthis, K and Janeček, M, (2017) Influence of equal channel angular pressing temperature on texture, microstructure and mechanical properties of extruded AX41 magnesium. J. Alloys Comp. 705: 273–282.
12. Hess, JB and Barrett, CS, (1949) Structure and Nature of Kink Bands in Zinc. T. Am. I. Min. Met. Eng. 185: 599–606.